Growth Mode and Electronic Structure of Au Nano-clusters on NiO(001) and TiO_2(110)

T. Okazawa[1], M. Fujiwara[2], T. Nishimura[2], T. Akita[1], M. Kohyama[1] and Y. Kido[2]

Abstract

The growth mode and electronic structure of Au nano-clusters grown on NiO and TiO_2 were analyzed by reflection high-energy electron diffraction, a field-emission type scanning electron microscope, medium energy ion scattering and photoelectron spectroscopy. Au was deposited on clean NiO(001)-1×1 and TiO_2(110)-1×1 surfaces at room temperature with a Knudsen cell at a rate of 0.25 – 0.35 ML/min (1 ML = 1.39×10^{15} atoms/cm^2 : Au(111)). Initially two-dimensional (2D) islands with thickness of one Au-atom layer grow epitaxially on NiO(001) and then neighboring 2D-islands link each other to form three-dimensional (3D) islands with the c-axis oriented to the [111] direction. The critical size to form 3D-islands is estimated to be about 5 nm^2. The shape of the 3D-islands is well approximated by a partial sphere with a diameter *d* and height *h* ranging from 2.0 to 11.8 nm and from 0.95 to 4.2 nm, respectively for Au coverage from 0.13 to 4.6 ML. The valence band spectra show that the Au/NiO and Au/TiO_2 surfaces have metallic characters for Au coverage above 0.9 ML. We observed Au 4f spectra and found no binding energy shift for Au/NiO but significant higher binding energy shifts for Au/TiO_2 due to an electron charge transfer from Au to TiO_2. The work function of Au/NiO(001) gradually increases with increase in Au coverage from 4.4 eV (NiO(001)) to 5.36 eV (Au(111)). In contrast, a small Au deposition(0.15 and 1.5 ML) on TiO_2(110) leads to reduction of the work function, which is correlated with an electron charge transfer from Au to TiO_2 substrate.

---

[1] *Advanced Industrial Science and Technology, AIST, Ikeda, Osaka 563-8577, Japan*

[2] *Department of Physics, Ritsumeikan University, Kusatsu, Shiga-ken 525-8577, Japan*

1. Introduction

Since Haruta et al.[1] found that nano-size clusters of Au deposited on oxide supports (for example, TiO_2, Fe_2O_3, Co_3O_4 and NiO for CO oxidation) exhibit high catalytic activities, a lot of works[2-6] have been reported in particular, on Au nano-particles supported on TiO_2. Valden et al.[7] showed that a quantum size effect of catalytic oxidation of carbon-mono-oxide (CO) molecules on TiO_2. Islands consisting of two layers of Au exhibit a band gap of 0.2 to 0.6 eV and are most effective for catalyzing the oxidation. Up to now, it is generally believed that the catalytic activities of Au nano-clusters depend on their size and independent of the support materials. Recently, however, Liu et al.[8] performed the first principles calculations for oxidation of CO adsorbed on Au/TiO_2(110) and showed that positively charged Ti at the interface enhances electron transfer from the supported Au to adsorbed O_2 and thus O_2 is highly activated. Similar charge transfer from Au to adsorbed O_2 was also predicted by Molina et al.[9]. More recently, Okazaki et al.[10] also claimed that the catalytic activity of Au nano-particles on TiO_2 cannot be explained only by the size effect and the charge transfer takes place from Au to O atoms at the Au/TiO_2(110) interface due to the orbital hybridization. Such a charge transfer probably changes the electronic states of the Au nano-particles and it may be correlated with the catalytic activities. So, it is of great interest to prepare well defined nano-clusters on a different oxide support and to clarify the correlation of the electronic states with the catalytic activity.

In this study, we prepared a clean NiO(001)-1×1 surface onto which Au was deposited by molecular beam epitaxy with Au coverage from 0.1 up to 9 ML (1 ML = 1.39×10^{15} atoms/cm^2, corresponding to the areal density of Au(111)). Small lattice mismatch of 2.4 % may lead to formation of epitaxial two-dimensional (2D) islands with a nm size. For comparison, Au nano-clusters were also grown on a clean TiO_2(110)-1×1 surface. The growth mode and electronic structure of Au/NiO and Au/TiO_2 were analyzed *in situ* by high-resolution medium energy ion scattering (MEIS) and photoelectron spectroscopy using synchrotron-radiation light. Reflection high energy electron diffraction (RHEED) provided the information about the crystallinity and morphology of the deposited Au. The shape and the areal occupation ratio of Au nano-clusters were observed *ex situ* by a field-emission type scanning electron microscope (FE-SEM) with an excellent spatial resolution better than 1 nm.

2. Experiment

The experiment was performed mainly at Beam-Line 8 named SORIS constructed at Ritsumeikan SR Center, which consists of photoelectron spectroscopy (PES), high-resolution MEIS and sample preparation systems. Clean NiO(001)-1×1 surfaces were prepared by annealing at 500˚C for 40 min in O_2-pressure of 1×10^{-4} Torr (base pressure: 3×10^{-10} Torr). RHEED observation showed a clear (1×1) pattern and Auger electron spectroscopy confirmed no carbon

contamination on the surface. No significant peak in the band gap originating from O-vacancies was observed in the valence band spectra taken at a photon energy of 40 eV. The image observed *ex situ* by an atomic force microscope (AFM) showed a smooth surface with flat terraces, although step bunching was seen in some places. We also prepared clean TiO_2(110) surfaces by sputtering with 0.75 keV Ar^+ followed by annealing at 550ºC for 5 min in O_2-pressure of 1×10^{-6} Torr. The RHEED observation showed a 1×1 pattern and the valence band spectra indicated no clear peak due to O-vacancies in the band gap indicating almost stoichiometric surface. After surface cleaning Au was deposited at room temperature on the clean surface using Knudsen cell at a rate of 0.25-0.35 ML/min.

The absolute amount of Au deposited was determined by MEIS using 120 keV He^+ ions with an accuracy better than 0.01 ML. Its excellent energy resolution allows a layer-by-layer analysis. As shown later, MEIS analysis also gives the quantitative information on the shape and the areal occupation ratio of Au islands. The 2D-images of the surfaces observed by FE-SEM check the validity of the above MEIS analysis. In order to avoid any effects changing the surface structure, we shifted an ion-irradiation area after an integrated beam current of 1 μC. In fact, the MEIS spectra did not change significantly after He^+-irradiation of ~5 μC. The growth mode and crystallinity of the deposited Au were monitored by RHEED. In addition, quite complementally photoelectron spectroscopy provides the information about the electronic structure of the Au/NiO and Au/TiO_2 surfaces. In the present analysis, we observed the valence band and Au 4f core level spectra using synchrotron-radiation light. The work functions of Au/NiO(001) and Au/TiO_2(110) were also determined by the photoemission spectra from the sample negatively biased. The incident photon energies were calibrated precisely using the 2nd and 3rd harmonic waves. All the above analyses were performed *in situ* under ultra-high vacuum condition ($\leq 2\times10^{-10}$ Torr), except for the FE-SEM observation.

3. Results and discussions

3-1. Growth mode

Figures 1 shows the MEIS spectrum observed for 120 keV He^+ ions incident along the [011] axis and backscattered to the $[0\,1\,\bar{1}]$ direction of NiO(001) for Au coverage of 1.4 ML.

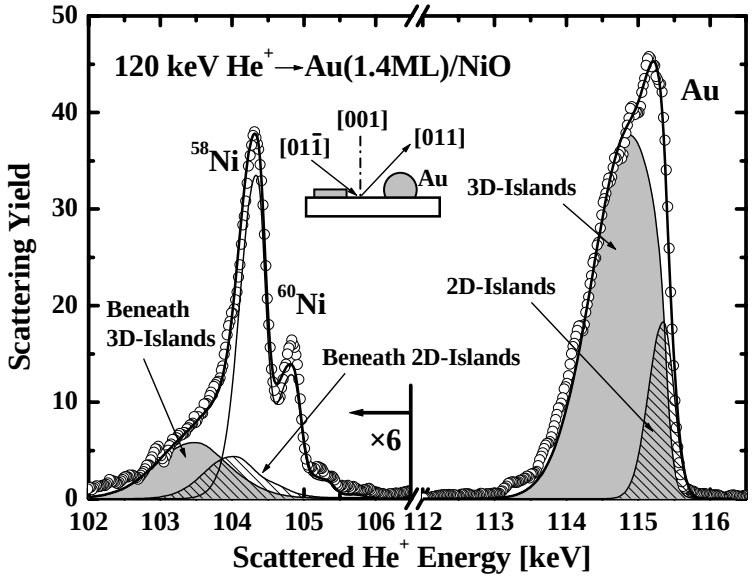

FIG. 1. MEIS spectrum observed for 120 keV He^+ ions scattered from Au and Ni of Au(1.4 ML)/NiO(001). He^+ ions were incident along the [011]-axis and backscattered to the $[01\bar{1}]$ direction of NiO(001). Thick curve denotes the total MEIS spectrum best-fitted to the observed one assuming d = 3.5 nm, h = 2.0 nm, σ_{2D}= 16 % and σ_{3D} = 26 %. The spectrum from Au clusters is decomposed into two components from 2D-islands(shaded) and 3D-islands(grey) and that from Ni has three components from the NiO substrate uncovered, beneath the 2D-islands (shaded) and 3D-islands(grey).

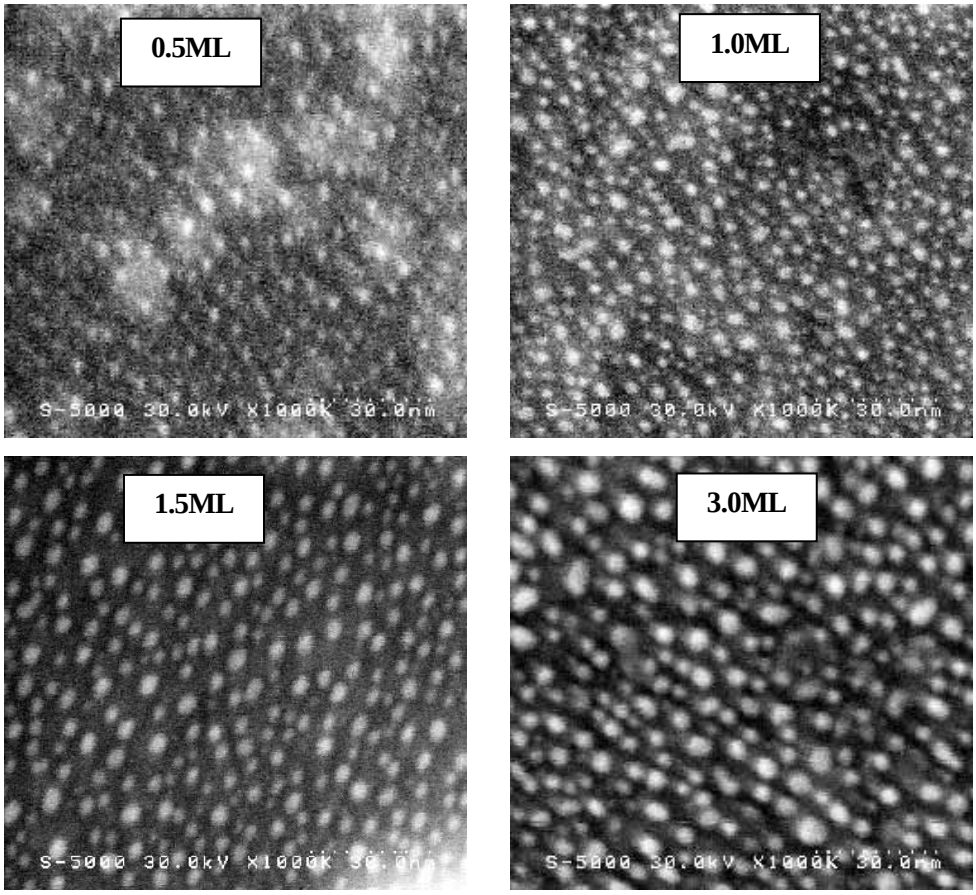

FIG. 2. FE-SEM images taken for Au coverage of 0.5, 1.0, 1.5 and 3.0 ML. The size of the images is 120 nm by 120 nm.

The observed scattering components from Ni and Au are best-fitted assuming that the surface is covered with 2D-islands with a height of one atomic layer and 3D-islands of a partial sphere with a mean diameter of d and height of h. Other fitting parameters are the areal occupation ratios of the 2D- and 3D-islands, σ_{2D} and σ_{3D}, respectively. The observed MEIS spectra are well reproduced assuming $d = 3.5 \pm 0.3$ nm, $h = 2.0 \pm 0.2$ nm, $\sigma_{2D} = 16 \pm 2$ % and $\sigma_{3D} = 26 \pm 3$ %. It must be noted that any disk-like shapes of 3D-islands cannot reproduce the observed MEIS spectra. In order to confirm the validity of the above MEIS analysis, we observed the surfaces by FE-SEM using 30 keV electron beams. The images taken for Au coverage of 0.5, 1.0, 1.5 and 3.0 ML are indicated in Fig. 2. The island size becomes gradually larger with increasing the Au coverage, although the image for Au coverage of 0.5 and 1.0 ML are not very clear. The island sizes for Au coverage of 1.5 and 3.0 ML range mainly from 3 to 4 nm and from 4 to 6 nm, respectively. This is consistent with the MEIS analysis.

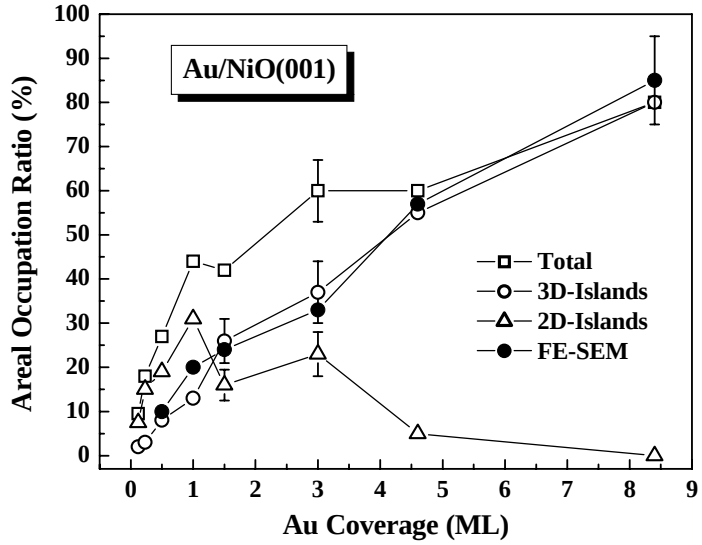

FIG. 3. Areal occupation ratios of σ_{2D} (open triangles) and σ_{3D} (open circles) together with the sum (open squares) as a function of Au coverage. The occupation ratios estimated from FE-SEM images are depicted by full circles.

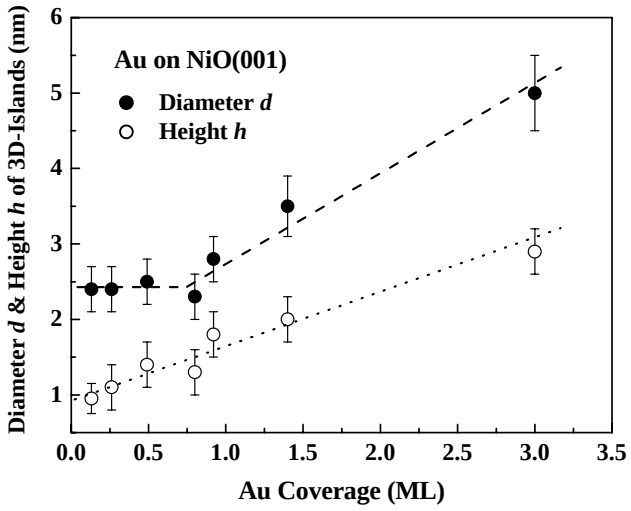

FIG. 4. The diameter d and height h of Au 3D-islands on NiO(001) determined by MEIS as a function of Au coverage.

The areal occupation ratios of 2D-, 3D-islands and the sum determined by MEIS are shown as a function of Au coverage in Fig. 3. The occupation ratios of the clusters observed by FE-SEM are compared with the result of MEIS. The σ_{3D} values as a function of Au coverage coincide with the occupation ratios of clusters in the FE-SEM images. This indicates that only 3D-islands are visible in the FE-SEM images. It is also seen that the formation of 2D-islands dominates in the initial

stage up to Au coverage of 1.0 ML and then 3D-islands start to grow later. The 3D-islands coalesce and the 2D-islands disappear for Au coverage above 5 ML. Figure 4 shows the d and h values determined by MEIS as a function of Au coverage. The diameter of 3D islands is almost constant (2.4 ~ 2.8 nm) for Au coverage from 0.13 up to 0.75 ML within experimental errors. In contrast, the height h and the occupation ratio σ_{3D} gradually increase with increasing Au coverage up to 3.0 ML. The above facts suggest a lateral critical size of about 5 nm^2 to change the growth mode from 2D- to 3D-islands. The significant reduction of σ_{2D} at Au coverage of 1.4 ML is probably due to the presence of such a critical size. The present analysis clarifies the fact that the critical size governs the growth mode of Au clusters on NiO(001) rather than critical Au coverage. If the size of 2D-islands exceeds the critical one, growth of 3D-islands becomes more stable energetically because the spherical shape reduces the surface energy.

The crystallinity and orientation of Au clusters were analyzed by RHEED. Figure 5 shows the RHEED patterns observed at the [110]- and [130]-azimuth for the NiO(001) surface deposited with 1.0 ML Au. It is seen that the surface is covered partly with two types of 2D-islands of Au(111), (i) Au[110]//NiO[110] and (ii) Au[$11\bar{2}$]//NiO[110]. The lateral crystal axes of the two types of domains make an angle of 30º. Crystalline 3D-islands were observed for Au coverage above 1.4 ML (σ_{2D} = 16 %, σ_{3D} = 26 %). The [110] and [112] diffractions appear as streaks at all the azimuth, indicating formation of 3D-islands with a c-axis oriented to the [111]-direction, probably due to the close packed plane. Thus the MEIS spectra observed for He^+ ions scattered from Au clusters are random, as shown previously.

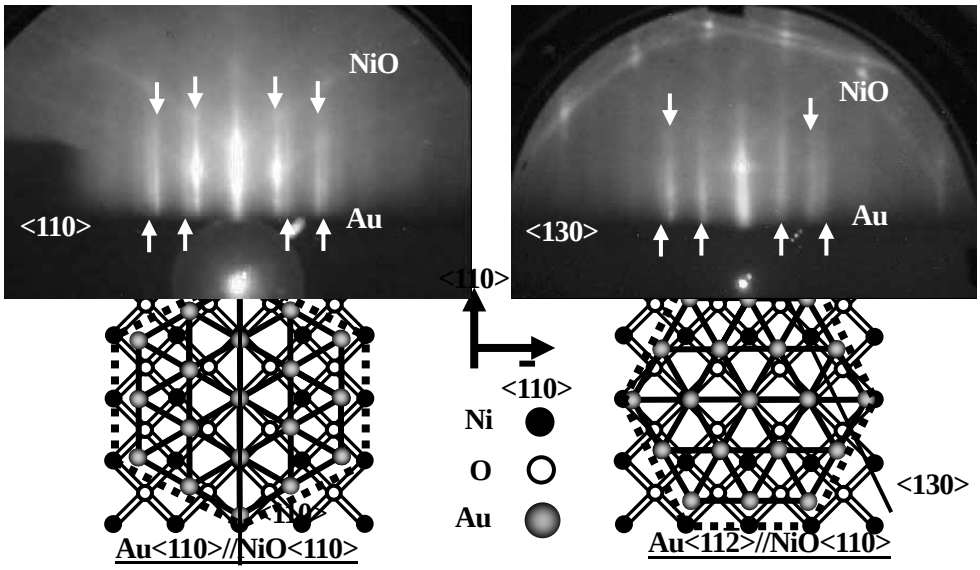

FIG. 5. RHEED images observed at the [110]- and [130]-azimuth for Au(1.0 ML)/NiO(001).

It is interesting to compare the growth mode of Au/NiO(001) with that of Au/TiO_2(110). Figure 6 shows the MEIS spectra observed for 120 keV He^+ ions incident along the [100] axis and backscattered to the [010]-direction of TiO_2(110) with Au coverage of 0.1, 0.2, 0.46 and 0.7 ML. In contrast to the Au clusters on NiO(001), all the Au clusters on TiO_2(110) for Au coverage above 0.7 ML are 3D-islands whose c-axis is not well oriented. This is probably due to a large lattice mismatch between Au and TiO_2(110). Parker et al.[4] reported that the onset of 3D island growth corresponds to Au coverage of 0.086 ML and the occupation ratios of Au islands are ~13 and ~22 %, respectively for Au coverage of 0.25 and 0.7 ML on the stoichiometric TiO_2(110) surface at 293 K. The present MEIS result is consistent with the above observation. The shape and size of the 3D-islands are compatible with those of the 3D-islands on NiO(001), for example, d = 2.8(2.4) nm and h = 1.4(1.1) nm and d = 4.7(5.0) nm and h = 3.4(2.9) nm for Au coverage of 0.25 and 2.5 ML, respectively (parentheses : Au/NiO).

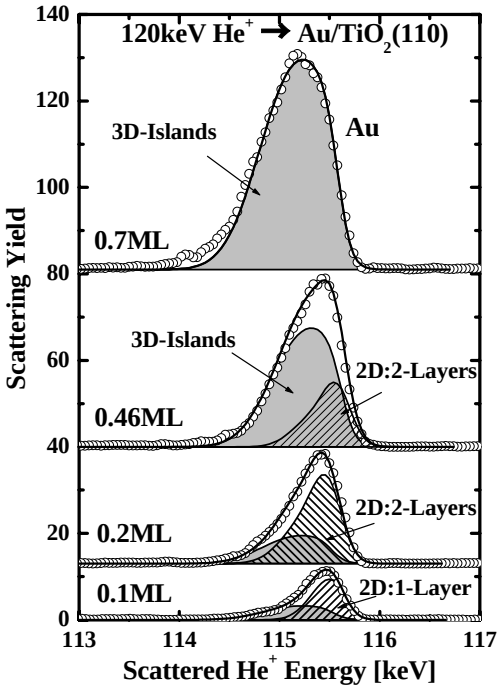

FIG. 6. MEIS spectra observed for 120 keV He^+ ions incident along the [100]-axis and backscattered to the [010] direction of TiO_2(110). The scattering components from 2D-islands are depicted by shaded areas and those from 3D-islands are indicated by grey areas. The thickness of 2D-islands is assumed to be one Au-atom layer for Au coverage of 0.1 ML and two Au-atom layers for Au coverage of 0.2 and 0.46 ML. Fitting parameters (d, h, σ_{2D}, σ_{3D}) assumed are (2.8 nm, 1.4 nm, 6.2 % , 1.3 %), (2.8 nm, 1.4 nm, 7.2 % ,1.3 %), (2.8 nm, 1.4 nm, 6.0 % , 16 %) and (3.0 nm, 1.5 nm, 0 %, 19 %) for Au coverage of 0.1, 0.2, 0.46 and 0.7 ML, respectively.

3-2. Electronic structure

If we diminish the number of atoms in an agglomerate, the energy gap between occupied and unoccupied states increases to a value exceeding the thermal energy $k_B T$ (k_B: Boltzmann constant, T: absolute temperature). It is generally recognized that the number of atoms from 50 to several hundred is necessary to induce a transition from a metal cluster to an insulator. Valden et al.[7] reported that metal to nonmetal transition takes place at a cluster size of 3.5 nm in diameter and 1.0 nm in height, corresponding to about 300 atoms/cluster. Recently, Okazaki et al.[10] showed that the mean inner potential of Au clusters determined by electron holography increases abruptly for the size below 5 nm. Such a dramatic change of the electronic structure is intimately related to the catalytic activity. So, it is of great importance to analyze the electronic structure dependent on the size and shape of Au clusters.

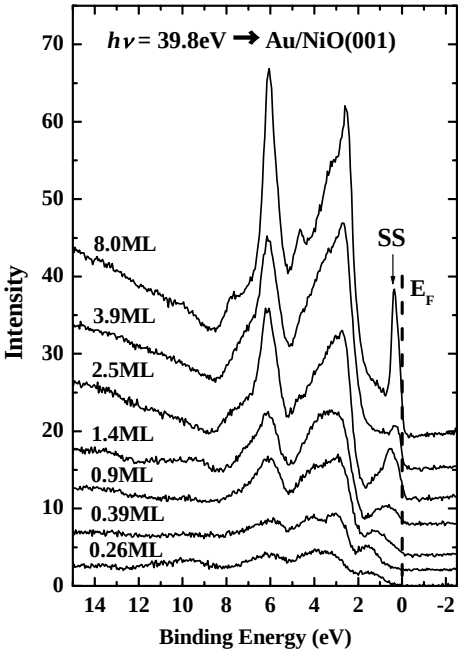

FIG. 7. Valence band spectra taken at photon energy of 39.8 eV for NiO(001) surfaces deposited with Au (0.26, 0.39, 0.9, 1.4, 2.5, 3.9 and 8 ML). Detection angle was set to surface normal. The abscissa indicates the binding energy scaled from the Fermi level. The spectra indicated here are obtained by subtracting the spectrum measured for clean NiO(001) surface.

Figure 7 shows the valence band spectra taken at photon energy of 39.8 eV under normal emission condition. As clearly seen, the surface becomes metallic for Au coverage above 0.9 ML, where the sum of the areal occupation ratios of 2D- and 3D-islands are 45 %. We observed the Shockley surface state (SS) ~0.5 eV below the Fermi level for Au coverage above 2.5 ML which appears for Au(111) surface[11]. In the case of Au/TiO_2(110), the surface has a

metallic character for Au coverage above 0.9 ML and the Shockley surface state peak was observed for Au coverage above 8 ML. The valence band spectra observed for Au/NiO(001) are basically similar to those for Au/TiO_2(110).

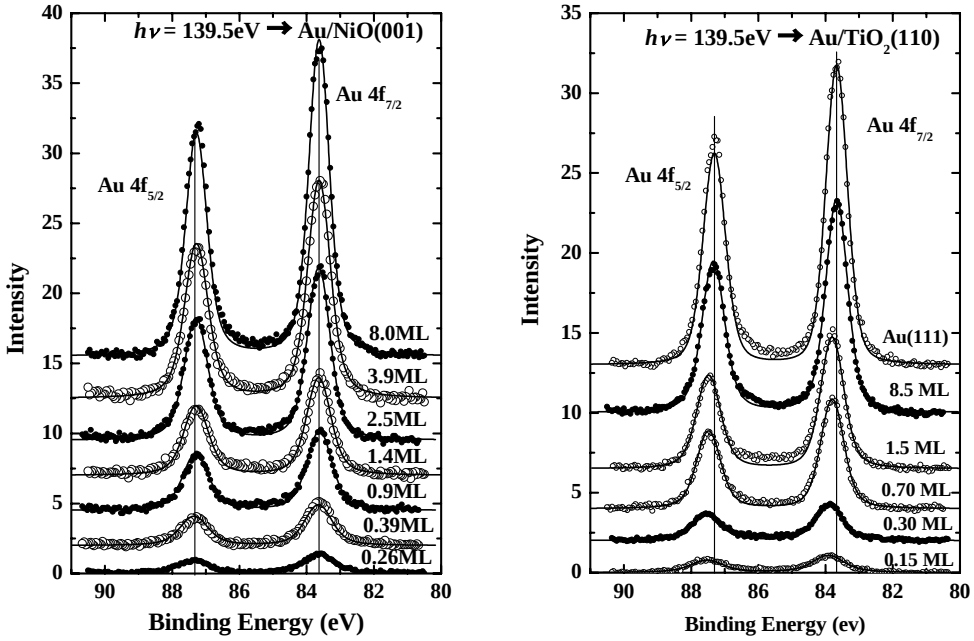

FIG. 8. (a) Au $4f_{5/2,7/2}$ core level spectra measured at photon energy of 139.5 eV for Au on NiO(001) as a function of Au coverage. (b) Au $4f_{5/2,7/2}$ spectra observed for Au on TiO_2(110) as a function of Au coverage. For comparison, the spectrum observed for a single crystal Au(111) is also depicted. Emitted photoelectrons were detected at 0°(surface normal).

We observed the Au $4f_{5/2,7/2}$ core level spectra at photon energy of 139.5 eV for Au/NiO(001) as a function of Au coverage, which are shown in Fig. 8(a). It is clearly seen that there is no binding energy shifts. Figure 8(b) indicates the Au $4f_{5/2,7/2}$ spectra observed for Au/TiO_2(110). We find higher binding energy shifts of 0.2 – 0.3 eV with decreasing Au coverage from 8.5 ML down to 0.15 ML. This is consistent with the data for Au/TiO_2(110) surfaces with O-vacancies reported by Howard et al.[12]. The smaller binding energy shifts observed in the present analysis compared with the above data are ascribed to considerably smaller density of O-vacancies of the TiO_2 substrates prepared here. Such a higher binding energy shift may be caused by an electron charge transfer from Au to TiO_2 substrate via hybridization at the interface[10]. The degree of the charge transfer is probably different for stoichiometric and nonstoichiometric TiO_2(110) surfaces[10]. Howard et al.[12] tried to explain the higher binding energy shifts based on the effect of the positive charge left on the Au cluster immediately after a photoelectron emission but could not reproduce well the core level shifts and the midpoint energy of the photoemission threshold. No binding

energy shifts observed for Au/NiO(001) indicates no charge transfer from Au to NiO substrate. Masi et al.[13] observed the Au 4f and Ni 2p spectra for Au(1.5 nm)/NiO(001) and found no binding energy shift for Au 4f but a slight reduction (Ni^0) of Ni^{2+} at the interface. It is not clear at the present that the interface structure of Au-nano-cluster/NiO is different from that of Au-film/NiO.

We determined the work functions (Φ) for Au/NiO(001) and Au/TiO_2(110) surfaces. The sample was negatively biased ($-V$) and the energy spectrum of the emitted photoelectrons was observed[14]. Figure 9 shows the yield of photoelectrons including secondary electrons as a function of $E_k - V + \Phi_{SP}$. Here, E_k and Φ_{SP} are the kinetic energy of the emitted electrons and the work function of the spectrometer, respectively. The yield of the photoelectrons was normalized by integrated photo-current. If the cut-off kinetic energy of photoelectrons ($E_{kin}^{\ 0}$) is observed, the work function is given by

$$\Phi = E_{kin}^{\ 0} - V + \Phi_{SP}. \quad (1)$$

The work function of the spectrometer Φ_{SP}(3.84 eV) can be determined from the following relation.

$$\Phi_{SP} = h\nu + V - E_{kin}^{\ F}, \quad (2)$$

where $E_{kin}^{\ F}$ is the Fermi edge (we used Au foils as a target) and $h\nu$ is an incident photon energy. The work functions for Au/NiO(001) and Au/TiO_2(110) are shown in Figs. 10(a) and (b), respectively as a function of Au coverage. The work function gradually increases from 4.41 (NiO) to 5.36 eV (Au(111)) with increasing Au coverage from 0 up to 8.0 ML. Such a gradual increment of the work function with increase in Au coverage is correlated with the areal occupation ratio of the Au islands (see Fig. 3) and this is quite reasonable because the electrostatic potential exerted on an electron near the surface is averaged over the contributions from the NiO(001) and Au nano-clusters surfaces.

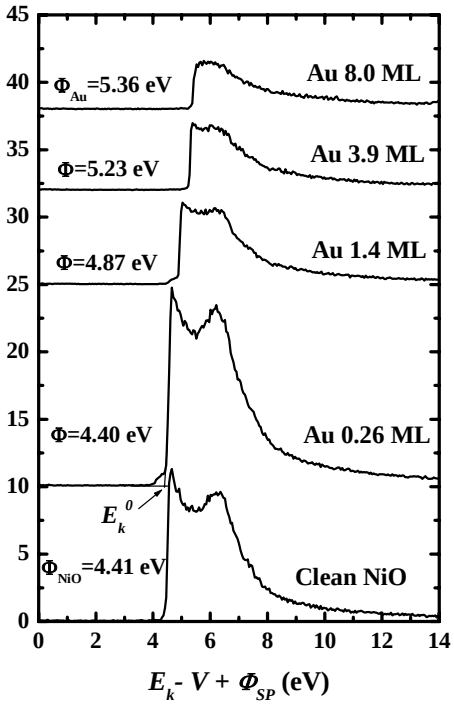

FIG. 9. Photoelectrons yield measured for Au/NiO(001) as a function of $E_k - V + \Phi_{SP}$. Here, the incident photon energy and the bias voltage applied were 20.0 eV and –7.69 V, respectively and photoelectrons were detected in the surface normal direction. The yield of photoelectrons was normalized by an integrated photo-current.

In the case of Au/TiO_2(110), however, the difference between the work functions of Au and TiO_2(110) is very small (0.13 eV). The work function observed as a function of Au coverage varies quite differently from that of Au/NiO. Remarkable drop of the work function by Au deposition of 0.15 – 1.5 ML is correlated to an electron charge transfer taking place from Au to TiO_2 substrate, which is evidenced from the higher binding energy shifts of Au 4f for Au coverage of 0.15 and 1.5 ML. Here, we must note that an electric filed generated on the vacuum side acts on emitted electrons and the work done against the field from the top surface to a region far from the surface corresponds to the work function. The reason is not clear why the work function of Au(0.15 to 1.5 ML)/TiO_2(110) becomes lower than clean TiO_2(110) and bulk Au. As a probable mechanism, the interface dipole induced by electron charge transfer from Au to TiO_2 reduces the work function. The electric field generated by the interface dipole is screened completely by thick Au over-layers for Au coverage above 8 ML (the areal occupation ratio of Au is more than 80 %).

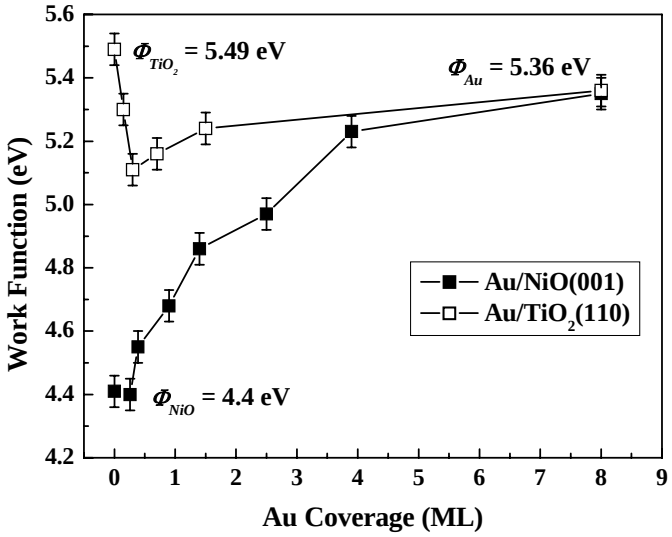

FIG. 10. Work functions determined by photoemission spectra for Au/NiO(001) (full squares) and Au/TiO_2(110) (open squares) as a function of Au coverage.

The present analysis shows that Au nano-clusters with a nearly same size and shape (partial sphere) are grown on NiO(001) and TiO_2(110) but the electronic structure of the Au/NiO(001) is significantly different from that of the Au/TiO_2(110). According to the report of Haruta[1], the catalytic activity of the Au/NiO(001) for CO oxidation is similar to that of the Au/TiO_2(110). So, it is not clear whether the electronic structure of Au/oxide-support is correlated with the catalytic activity. Systematic data accumulation of electronic and morphological structures of Au/metal-oxide is strongly required.

4. Summary

We have unveiled the growth mode and electronic structure of Au nano-clusters grown on NiO(001) and TiO_2(110) by RHEED, FE-SEM, MEIS and photoelectron spectroscopy using synchrotron-radiation light. Au was deposited on clean NiO(001)-1×1 and TiO_2(110)-1×1 surfaces at room temperature with a Knudsen cell at a rate of 0.24 ML/min. Initially 2D- islands with thickness of one Au-atom layer grow epitaxially on NiO(001) and then neighboring 2D-islands link each other to form 3D-islands with the c-axis oriented to the [111] direction. The critical size to form 3D-islands is estimated to be about 5 nm^2. The 2D-islands of Au(111) take two types of domains, Au[110]//NiO[110] and Au[$11\bar{2}$]// NiO[110]. The 2D-islands disappear for Au coverage above 7 ML. The shape of the 3D-islands is well approximated by a partial sphere with a diameter *d* and height *h*. With increasing Au coverage the average *d* and *h* values increase gradually. In contrast to the Au clusters on NiO(001), all the Au clusters on TiO_2(110) for Au coverage above 0.7

ML are 3D-islands whose c-axis is not well oriented. The valence band spectra show that the Au/NiO and Au/TiO_2(110) surfaces have metallic characters for Au coverage above 0.9 ML. The valence band spectra observed for Au/NiO(001) are basically similar to those for Au/TiO_2(110). We found significant higher binding energy shifts of Au 4f for Au/TiO_2 but not for Au/NiO. Such a higher binding energy shift suggests an electron charge transfer from Au to TiO_2 substrate. The work function of Au/NiO(001) gradually increases with increasing Au coverage from 4.4 eV (NiO(001)) to 5.36 eV (Au(111)). This is responsible for the fact that the electrostatic potential exerted on an electron near the surface is averaged over the contributions from the NiO(001) and Au nano-clusters surfaces. On the other hand, Au deposition from 0.15 to 1.5 ML on TiO_2(110) leads to reduction of the work function. This is correlated to an electron charge transfer from Au to TiO_2 substrate, which is evidenced by higher binding energy shifts of Au 4f.

Acknowledgements

The authors would like to thank Prof. H. Namba and Dr. K. Ogawa for maintaining the Beam-Line 8 at Ritsumeikan SR Center. They are debt to Ms. M. Makino in FE-SEM observation at AIST. Thanks are also due to our colleagues, Dr. Y. Hoshino and Mr. T. Nishizawa for their help in carrying out the PES and MEIS analyses.

References

[1] M. Haruta, N. Yamada, T. Kobayashi and S. Iijima, J. Catal. **115** (1989) 301.

[2] Y. Iizuka, H. Fujiki, N. Yamauchi, T. Chijiiwa, S. Arai, S. Tsubota and M. Haruta, Catal. Today **36** (1997) 115.

[3] C. Xu, W.S. Oh, G. Liu, D.Y. Kim and D.W. Goodman, J. Vac. Sci. Technol. **A 15** (1997) 1261.

[4] S.C. Parker, A.W. Grant, V.A. Bondzie and C.T. Campbell, Surf. Sci. **441** (1999) 10.

[5] H.J. Freund, Surf. Sci. **500** (2002) 271.

[6] T. Minato, T. Susaki, S. Shiraki, H.S. Kato, M. Kawai and K. Aika, Surf. Sci. **566-568** (2004) 1012.

[7] M. Valden, X. Lai and D.W. Goodman, Science **281** (1998) 1647.

[8] Z-P. Liu, X-Q. Gong, J. Kohanoff, C. Sanchez and P. Hu, Phys. Rev. Lett. **91** (2003) 266102.

[9] L.M. Molina, M.D. Rasmussen and B. Hammer, J. Chem. Phys. **120** (2004) 7673.

[10] K. Okazaki, S. Ichikawa, Y. Maeda, M. Haruta and M. Kohyama, Appl. Catal. **A 291** (2005) 45.

[11] S. Hüfner, *Photoelectron Spectroscopy* (Springer-Verlag, New York, 1996).

[12] A. Howard, D.N.S. Clark, C.E.J. Mitchell, R.G. Egdell and V.R. Dhanak, Surf. Sci. **518** (2002)

210.
[13] R. de Masi, D. Reinicke, F. Müller, P. Steiner and S. Hüfner, Surf. Sci. **515** (2002) 523.
[14] T. Nishimura, J. Takeda, Y. Asami, Y. Hoshino and Y. Kido, Surf. Sci. **588** (2005) 71.